PHILOSOPHICAL TRANSACTIONS OF THE ROYAL SOCIETY A
MATHEMATICAL, PHYSICAL & ENGINEERING SCIENCES

A Thermodynamical Theory of Turbulence II. Determination of Constitutive Coefficients and Illustrative Examples

J. S. Marshall and P. M. Naghdi

Phil. Trans. R. Soc. Lond. A 1989 **327**, 449-475
doi: 10.1098/rsta.1989.0002

Phil. Trans. R. Soc. Lond. A **327**, 449–475 (1989) [449]
Printed in Great Britain

A THERMODYNAMICAL THEORY OF TURBULENCE II. DETERMINATION OF CONSTITUTIVE COEFFICIENTS AND ILLUSTRATIVE EXAMPLES

By J. S. MARSHALL and P. M. NAGHDI
Department of Mechanical Engineering, University of California, Berkeley, California 94720, *U.S.A.*

(*Communicated by A. E. Green, F.R.S. – Received* 25 *August* 1987 – *Revised* 4 *December* 1987)

CONTENTS

	PAGE
1. Introduction	450
2. On direct measurements of additional turbulence variables on the microscopic scale	451
2.1. A simplified model of the microscopic flow	452
2.2. Measurement of turbulent temperature	454
2.3. Measurement of eddy density	455
2.4. Measurement of the director	455
3. Simplified equations for incompressible viscous turbulent flow	456
4. Determination of the constitutive coefficients	459
4.1. Dissipation of turbulence	459
4.2. Production of eddies	460
4.3. Diffusion of thermal heat and turbulent fluctuations	462
4.4. Coefficients in the expression for free energy	463
4.5. Viscosity coefficients	463
5. Solutions for some simple turbulent flow problems	464
5.1. Flow possessing a constant uniform velocity gradient	464
5.2. Decay of ‘anisotropy’ with vanishingly small velocity gradient	465
5.3. Plane turbulent channel flows	467
5.4. Solution for turbulent plane Poiseuille flow in a two-dimensional channel	469
6. Concluding remarks	474
References	475

This paper is a continuation of Part I under the same title and is concerned mainly with the determination of the constitutive response coefficients, as well as some simple illustrative examples. First, a system of simplified constitutive equations for incompressible viscous turbulent flow is obtained from the more general system of equations in Part I through a judicial choice of retaining only those terms which appear to represent major features of the turbulent flow. Even for this simplified system of equations, the identification of some of the constitutive coefficients presents a formidable task; and this is especially true in the case of those coefficients that are

31-2

associated with the presence of the additional independent variables of the theory due to the manifestation of the alignment of eddies (on the microscopic scale), turbulent fluctuation and eddy density. Because of this difficulty, the present effort for identification of the various constitutive coefficients must be regarded partly as tentative, pending future availability of suitable relevant experimental data and/or pertinent numerical simulation results. Keeping this background in mind, most of the relevant coefficients in the constitutive equations are determined, or the nature of their functional forms are estimated, through consideration of 'cartoon-like' *models* on the microscopic level and these results are then used in conjunction with the macroscopic equations of motion to examine a number of simple solutions. These include the possibility of a flow possessing a constant uniform velocity gradient and solutions pertaining to decay of flow anisotropy and plane turbulent channel flows. The predicted theoretical calculations are in general accord with experimental observations. In addition, for plane channel flow, plots of variation along the width of the channel for the turbulent temperature and the macroscopic velocity compare favourably with corresponding known experimental results.

1. Introduction

This paper is a companion to Part I under the same title (hereafter referred to as I), which contains the basic developments for a thermodynamical theory of turbulent fluid flow. The purpose of the present paper is to provide a number of simplifications of the basic theory in I, necessary further identification between quantities defined on microscopic and macroscopic scales, determination of the various constitutive coefficients, and also illustrations for the use of the resulting equations by solving some simple turbulent flow problems. Determination of the functional forms of the constitutive response coefficients of the theory is required before the use of the turbulent flow equations in solving specific problems, and thus such identification necessarily constitutes a major portion of the present paper.

In I, a theory based on a continuum model of turbulence is formulated on the macroscopic (bulk) scale which employs certain additional independent variables and associated balance laws to describe particular features occurring on the microscopic (turbulent) and molecular scales. These additional variables include the turbulent temperature θ_T, the eddy density ρ_E and the director $\boldsymbol{d}$, as well as the usual thermal temperature θ_H. A set of governing equations for turbulent fluid flow is then obtained (under certain plausible simplifying assumptions) with the use of the invariance requirements under superposed rigid body motions and the thermodynamical procedure of Green & Naghdi (1977), along with certain constraints placed upon the theory due to director alignment and the condition of incompressibility (when relevant).

A discussion pertinent to the direct measurement (from the microscopic scale) of the additional turbulence variables θ_T, ρ_E and $\boldsymbol{d}$ and including explicit identification of these variables with microscopic features (which is much more detailed than that given in I) is presented in §2. We emphasize that measurements of these additional turbulence variables in future experimental work is vital in order to properly compare quantitative predictions of the theory with these experimental results. A system of constitutive equations for an incompressible viscous turbulent flow, which are simpler than those derived previously and do not include several terms in the more general equations of I (§6), is recorded in §3. The physical significance of various terms in these simplified equations is examined and they seem to include all major features of turbulent flow.

In §4, we formulate 'cartoon-like' microscopic models (i.e. idealized microscopic flows derived from pictures of the flow structure based on experimental studies), which are used to obtain approximate functional forms for many of the response coefficients appearing in the simplified constitutive equations of §3. Some of these 'cartoon-like' models (however not all) yield results which correspond to similar estimates found in the turbulence literature (see, in particular, Perry & Chong (1982), Ahlborn *et al.* (1985) and Liu *et al.* (1985)), in which case the discussion is made as brief as possible. The resulting equations are then used in §5 to solve some simple problems that exhibit flow anisotropy. Included is a discussion of a flow possessing a constant uniform velocity gradient and solutions for the decay of 'anisotropy' in the absence of ordinary velocity gradient and plane turbulent channel flows. These theoretical solutions are found to possess appropriate functional forms, as well as predicted numerical calculations in the case of plane channel flow, which are supported by results of corresponding known experimental studies of Laufer (1951). Further comparison of these solutions with more detailed experimental results may allow for accurate determination of the constants of proportionality associated with certain constitutive coefficients; however, such identification is seriously hampered by the fact that two of the additional turbulence variables used here (namely ρ_E and d) cannot easily be estimated from the available data reported in these experimental studies, and hence only tentative estimates for these constants can be made. A quick summary of the basic microscopic features that, if measured, would enable reasonable estimates of ρ_E and d is given in §6.

2. On direct measurements of additional turbulence variables on the microscopic scale

Before the discussion pertaining to the direct measurement of additional turbulence variables ρ_E, θ_T, d, it is desirable to provide supplementary background between the macroscopic turbulent flow model introduced in I (§§4 and 5) and the actual microscopic turbulent flow. Thus, we recall that turbulent flows are composed, at the microscopic level, of a great number of swirling eddies and vortices. Although in reality the sizes and strengths of these eddies vary nearly continuously within a sufficiently large fluid volume, it is convenient for the purposes of modelling to consider a somewhat idealized structure. In such idealized turbulence, the eddies are allowed to vary in size only among a small number of discrete size levels. The various classifications of eddy sizes are typically defined such that eddies which have similar effects on the macroscopic flow are grouped together in a single class. A great deal of discussion can be found in the literature on the appropriate classifications of eddy sizes. (Appropriate quotations from this literature can be found in I, Appendix A.)

There seems to be fair (although perhaps not complete) agreement in this literature that a minimum of three size classifications of vortices (as described by Savill (1987, pp. 540, 541) and Townsend (1976, p. 105)) are needed to sufficiently describe a turbulent flow. These include the following classes:

(1) very large swirling motions (termed 'lasmos' by Savill (1987)) whose dimensions are roughly that of the macroscopic flow and whose orientations and strengths depend on the particular flow geometry in question (these vortices are roughly two-dimensional and tend to be located periodically in many flows);

(2) large eddies (termed 'roller eddies' by Savill (1987), 'main turbulent motion' by

Townsend (1976), 'hairpin' vortices by Head & Bandyopadhyay (1981), etc.), which are oriented and strained by the macroscopic flow (these eddies are significantly smaller than the 'lasmos,' yet they contain most of the 'hidden' turbulent kinetic energy);

(3) smaller eddies, which arise from the break-up of larger eddies and act to dissipate the turbulent energy into thermal heat.

Following Townsend (1976, p. 89), we assume that the rate of dissipation of turbulence is controlled only by the rate at which the large eddies of class (2) can pass energy down to the smaller eddies of class (3). Because on this assumption these small eddies control no feature of the macroscopic turbulent flow, we do not need to describe particular aspects of these eddies in the macroscopic theory. Additionally, several properties of the 'lasmos' type eddies of class (1), such as their size, two-dimensional form, and periodicity, indicate that these vortices represent (non-chaotic) solutions of the macroscopic turbulence equations, rather than a (chaotic) structure on the microscopic level. The validity of this assumption is especially evident for vortices that are in some way analogous to similar (non-chaotic) vortical solutions of the laminar flow equations (such as the vortex-street type vortices in wake flows or the large roller vortices in free shear layers). Other large (macroscopic) vortical motions may result from flow 'anisotropy' in certain shearing motions. (Such 'secondary' flows in turbulence are discussed in a recent review by Bradshaw (1987).)

We now recall from I (§§4 and 5) that certain features of the microscopic flow are already explicitly represented, with the use of the additional 'turbulence' variables ρ_E, θ_T and $\boldsymbol{d}$, in the macroscopic theory under consideration. In selecting these additional variables, our modelling has necessarily centred around the large eddies of class (2). For instance, the turbulent temperature θ_T represents the manifestation of the 'hidden' portion of the microscopic kinetic energy and, as already noted above, most of this kinetic energy may be associated with large eddies of class (2). Similarly, the eddy density ρ_E can be identified with the number of class (2) eddies per unit volume. The magnitude of the director $\boldsymbol{d}$ is proportional to the degree of 'vortex stretching' of class (2) eddies, and the direction of $\boldsymbol{d}$ is constrained to be the same direction as that along which class (2) eddies tend to become aligned. It may be noted that θ_T and ρ_E can be related to the more standard 'turbulent kinetic energy' and 'mixing length,' respectively, as will be shown presently in §§2.2 and 4.1. The main function of the director is to describe the degree and direction of flow 'anisotropy.' As such, the director may be expected to significantly affect the rate of entrainment of fluid at a turbulent–non-turbulent interface, the form of the stress tensor t_{ij} and the rate of production of turbulent fluctuations by the shearing of the macroscopic flow. As discussed in I (§8), the latter effect can occur both within the fluid and along a surface of discontinuity.

To provide more detailed identification of and to facilitate direct measurement of the additional turbulence variables ρ_E, θ_T and $\boldsymbol{d}$, we now provide a detailed discussion of each of these variables in the following subsections. Preliminary to such considerations, however, a simplified model for the microscopic flow is introduced which is then used to clarify the difference between the macroscopic flow and the 'mean' flow.

2.1. *A simplified model of the microscopic flow*

We consider here a simplified model of the microscopic flow in which every macroscopic point (in the current configuration) $\boldsymbol{x}$ is surrounded on the microscopic level by a (reasonably small) region $\mathscr{P}'$ and an additional directed line segment which we represent by a vector function of position and time and denote by $\boldsymbol{d} = \boldsymbol{d}(\boldsymbol{x}, t)$. (We use the same notation here as that in §5 of Part I, in anticipation of later identification of this directed line segment with the director on the macroscopic level (see I, equation (5.4)).) Here the directed line segment $\boldsymbol{d}$ is assumed to exist on a different dimensional space than the region $\mathscr{P}'$, so that taken together they constitute a four-dimensional region $\mathscr{P}^*$. Let λ be a parameter along $\boldsymbol{d}$ which varies in the interval $\mathscr{I} = (-\frac{1}{2}, \frac{1}{2})$, let $\boldsymbol{x}'$ be a typical point in the region $\mathscr{P}'$ and let the macroscopic point $\boldsymbol{x}$ be identified with the centre of mass of $\mathscr{P}^*$ corresponding to the point $(\boldsymbol{x}', \lambda) = (\mathbf{o}, 0)$. The microscopic location $\boldsymbol{x}^*$ $(\in \boldsymbol{P}^*)$ may then be specified as

$$\boldsymbol{x}^* = \boldsymbol{x} + \lambda \boldsymbol{d} + \boldsymbol{x}', \tag{2.1}$$

where the asterisk in (2.1) and elsewhere in this section is used to designate quantities belonging to the microscopic scale of motion. The velocity on the microscopic scale is

$$\boldsymbol{v}^* = \boldsymbol{v} + \lambda \boldsymbol{w} + \boldsymbol{v}', \tag{2.2}$$

where

$$\boldsymbol{v}^* = \dot{\boldsymbol{x}}^*, \quad \boldsymbol{v} = \dot{\boldsymbol{x}}, \quad \boldsymbol{w} = \dot{\boldsymbol{d}}, \quad \boldsymbol{v}' = \dot{\boldsymbol{x}}' \tag{2.3}$$

and (as in Part I) a superposed dot indicates differentiation with respect to t.

Letting $\mathrm{d}v^* \equiv \mathrm{d}v' \,\mathrm{d}\lambda$ be an element of the four-dimensional region $\mathscr{P}^*$, the velocity $\boldsymbol{v}$ of the centre of mass for an incompressible fluid (since the mass density is constant) must be such that

$$\frac{1}{\mathscr{V}^*}\int_{\mathscr{P}^*} \boldsymbol{v}^* \,\mathrm{d}v^* = \frac{1}{\mathscr{V}'}\int_{-\frac{1}{2}}^{\frac{1}{2}}\int_{\mathscr{P}'} \boldsymbol{v}^* \,\mathrm{d}v' \,\mathrm{d}\lambda$$

$$= \boldsymbol{v} + \frac{1}{\mathscr{V}'}\int_{\mathscr{P}'} \boldsymbol{v}' \,\mathrm{d}v' = \boldsymbol{v}, \tag{2.4}$$

where the hypervolume $\mathscr{V}^*$ and the volume $\mathscr{V}'$ occupy the regions $\mathscr{P}^*$ and $\mathscr{P}'$, respectively. The velocity $\boldsymbol{v}'$ may be referred to as the turbulent fluctuation velocity, and by $(2.4)_3$ must necessarily satisfy the condition

$$\int_{\mathscr{P}'} \boldsymbol{v}' \,\mathrm{d}v' = 0. \tag{2.5}$$

The microscopic kinetic energy per unit mass is $\kappa^* = \frac{1}{2}\boldsymbol{v}^* \cdot \boldsymbol{v}^*$ and its average over a volume $\mathscr{V}^*$ with the use of (2.2) can be calculated as follows:

$$\frac{1}{\mathscr{V}^*}\int_{\mathscr{P}^*} \kappa^* \,\mathrm{d}v^* = \frac{1}{\mathscr{V}^*}\int_{\mathscr{P}^*} \tfrac{1}{2} v_i^* v_i^* \,\mathrm{d}v^* = \kappa + \frac{1}{\mathscr{V}'}\int_{\mathscr{P}'} \tfrac{1}{2} v_i' v_i' \,\mathrm{d}v', \tag{2.6}$$

where

$$\kappa = \tfrac{1}{2}(v_i v_i + \tfrac{1}{12} w_i w_i). \tag{2.7}$$

and where in obtaining $(2.6)_2$ we have also used (2.4) and (2.5).

In view of the results (2.6) and (2.7), we are now in a position to identify the inertia coefficients y_1, y_2 which first appeared in the macroscopic kinetic energy introduced in I (§2). Thus, from a direct comparison of (2.7) with the previous expression for κ in I (equation (2.3)) we have

$$y_1 = 0, \quad y_2 = \tfrac{1}{12}. \tag{2.8}$$

As will become evident presently, we need to consider the question of what constitutes a definition for 'mean velocity' on the microscopic scale. Clearly such a definition can be introduced in a variety of ways, but for our present purpose we define a 'mean velocity' $\overline{v^*}$ by

$$\overline{\boldsymbol{v}^*} = \frac{1}{\mathscr{V}'}\int_{\mathscr{P}'} \boldsymbol{v}^*\,\mathrm{d}v' = \boldsymbol{v}+\lambda \boldsymbol{w}, \tag{2.9}$$

where (2.2) and (2.5) have been used in obtaining the second of (2.9). It should be noted that the definition $(2.9)_1$ is consistent with (2.4) and (2.5) in that the part of the velocity due to turbulent fluctuations does not contribute to the mean velocity $\overline{\boldsymbol{v}^*}$. Moreover, $(2.9)_2$ clearly shows that because of the additional structure included in the theory (in the form of the director $\boldsymbol{d}$) the velocity $\boldsymbol{v}$ is not identical to the 'mean' velocity $\overline{\boldsymbol{v}^*}$. However, in many flows the director velocity (but not necessarily the director itself) may be small compared to the velocity $\boldsymbol{v}$, in which case the 'mean' velocity $\overline{\boldsymbol{v}^*}$ may represent a sufficiently close approximation for $\boldsymbol{v}$.

While the effect of the microscopic line segment is averaged over the hypervolume $\mathscr{V}^*$ as in the case of (2.6) involving the microscopic velocity $\boldsymbol{v}^*$, because of the nature of the basic ingredients of our thermomechanical *model* for turbulence (see §§4 and 5 of I) for the effect of other microscopic variables such as the microscopic temperature θ^* and the mass density ρ^* it is sufficient to consider their averaged values only over the three-dimensional volume $\mathscr{V}'$. In particular, the macroscopic thermal temperature θ_{H} may be identified with the microscopic 'mean temperature' $\overline{\theta^*}$ defined by

$$\overline{\theta^*} = \frac{1}{\mathscr{V}'}\int_{\mathscr{P}'} \theta^*\,\mathrm{d}v' = \theta_{\mathrm{H}}. \tag{2.10}$$

Similarity, for a compressible fluid the macroscopic mass density ρ may be identified with the microscopic 'mean mass density' $\overline{\rho^*}$ defined by

$$\overline{\rho^*} = \frac{1}{\mathscr{V}'}\int_{\mathscr{P}'} \rho^*\,\mathrm{d}v' = \rho. \tag{2.11}$$

2.2. *Measurement of turbulent temperature*

The turbulent temperature θ_{T} is defined such that the 'mean' value of the microscopic kinetic energy per unit mass is related to the macroscopic kinetic energy κ and the turbulent temperature θ_{T} by

$$\frac{1}{\mathscr{V}^*}\int_{\mathscr{P}^*} \kappa^*\,\mathrm{d}v^* = \kappa + c_{\mathrm{T}}\,\theta_{\mathrm{T}}, \tag{2.12}$$

where c_{T} is the turbulent specific heat. It is at once apparent from comparison of (2.12) and (2.6) that

$$c_{\mathrm{T}}\,\theta_{\mathrm{T}} = \frac{1}{\mathscr{V}'}\int_{\mathscr{P}'} \tfrac{1}{2}v_i'\,v_i'\,\mathrm{d}v' \tag{2.13}$$

and we may then define c_{T} and θ_{T} as

$$c_{\mathrm{T}} = \frac{1}{a}, \quad \theta_{\mathrm{T}} = \frac{a}{\mathscr{V}'}\int_{\mathscr{P}'} \tfrac{1}{2}v_i'\,v_i'\,\mathrm{d}v', \tag{2.14}$$

where a is an arbitrary constant with the physical dimensions of temperature divided by the square of velocity. It should be clear that the definition $(2.14)_2$ is consistent with the assumption in I (§4) that θ_{T} must vanish as the turbulent fluctuations vanish. For definiteness, we choose the constant a as

$$a = 100\frac{{}^{\circ}T\,\mathrm{s}^2}{\mathrm{m}^2}, \tag{2.15}$$

where the abbreviations 's' and 'm' stand for seconds and metres, while one degree T is a measure of turbulent temperature defined through the specification (2.15). The value of a in (2.15) is chosen such that the resulting scale for turbulent temperature would be convenient in the range of experimental studies usually made. With the use of (2.14) and (2.15), values of θ_T can be obtained immediately from any of the various measurements of $1/\mathscr{V}' \int_{\mathscr{P}'} v_i' v_i' \, dv'$ found throughout the turbulence literature, i.e. from measurements of the usual turbulent kinetic energy'.

2.3. *Measurement of eddy density*

As discussed previously, the eddy density ρ_E is simply the number of large (class 2) eddies per unit volume of fluid. This definition is made, of course, with reference to the classification of turbulent eddies introduced at the beginning of this section. In an actual turbulent flow there is no clear distinction between the large (class 2) eddies and the small (class 3) eddies, but rather a fairly gradual transition in size. To directly measure the eddy density ρ_E, an instrument or procedure is required that can both count and identify the large (class 2) vortices. (Measurements of the common 'mixing length' also experience these difficulties.)

Supposing that a sufficient amount of information on the microscopic flow field is available (such as might be the case in computer simulated 'numerical experiments'), one must first establish a cut-off energy level that can be used to distinguish the large eddies (containing most of the microscopic kinetic energy) from the small eddies (containing only a negligible amount of microscopic kinetic energy). Such a cut-off is of the same nature as estimates of boundary layer thickness in laminar fluid flow. The number of eddies in a given volume possessing a net energy in excess of this cut-off value can then be counted, so that ρ_E is simply the number of such eddies divided by the volume that they occupy.

2.4. *Measurement of the director*

We recall from I (statement (5.4)) that the director magnitude is identified as being proportional to the difference in magnitude of the central microscopic vorticity vectors of the aligned and unaligned eddies times the ratio of number of large aligned eddies to the total number of large eddies. The microscopic vorticity vector $\boldsymbol{\omega}^*$ referred to here is obtained from the difference between the microscopic velocity $\boldsymbol{v}^*$ and the macroscopic velocity $\boldsymbol{v}$ as follows:

$$\boldsymbol{\omega}^* = \nabla \times (\boldsymbol{v}^* - \boldsymbol{v}). \tag{2.16}$$

A typical magnitude ω^* of $\boldsymbol{\omega}^*$ directed along the central axis of a large eddy is denoted by ω^a if the eddy is aligned in the direction $\boldsymbol{a}^3$ and by ω^0 otherwise. If we denote by f the ratio of number of large aligned eddies to the total number of large eddies contained in a (small) microscopic region $\mathscr{P}^*$ associated with a given macroscopic position $\boldsymbol{x}$, then the director must satisfy

$$\boldsymbol{d} \propto f(\omega^a - \omega^0)\, \boldsymbol{a}^3. \tag{2.17}$$

Further identification of the director must satisfy the stipulation that the average value of the kinetic energy on the microscopic level equals the macroscopic kinetic energy plus the part of the macroscopic internal energy due to turbulent fluctuations. This requirement is satisfied if we set

$$\frac{\boldsymbol{d}}{L} = \frac{f(\omega^a - \omega^0)}{\omega^0} \boldsymbol{a}^3, \tag{2.18}$$

where L is a unit length of the same dimensions as $\boldsymbol{d}(L = 1\,\text{cm}$, say). It may be recalled that for a potential fluid, the change of magnitude of the central vorticity vector of an eddy divided by its initial value is exactly equal to the stretch of a material line segment lying along the central axis of the eddy (Prandtl & Tietjens 1957, p. 200). In light of the identification (2.18), the magnitude of the director may be viewed as the net 'effective' stretch of the central vortical axes of large eddies contained in a certain microscopic region due to alignment of these eddies by the macroscopic flow. The qualifier 'effective' is used here to indicate that, because the flow is not potential and the circulation of the eddies is not necessarily constant, the actual stretch along the central axes of these eddies accompanying a given vorticity change might be considerably greater than indicated by (2.18).

Before measurement of the director, the principal direction $\boldsymbol{a}^3$ of the rate of deformation tensor along which the director is aligned must be identified at each macroscopic point $\boldsymbol{x}$. After measuring the central vorticity $\boldsymbol{\omega}^*$ for a range of eddies directed both along $\boldsymbol{a}^3$ and randomly in the fluid, estimates of ω^a and ω^0 can readily be made. However, the difficulties discussed previously in respect to direct measurements of ρ_E are even more acute in regard to measurements of f in (2.18), where we must not only identify the large eddies from the small eddies, but we must also distinguish the aligned eddies from the unaligned eddies. Despite these difficulties, it should be possible to obtain direct experimental estimates of ρ_E and $\boldsymbol{d}$ using modern experimental tools, especially in certain simplified special cases. In this regard, we note that 'pattern recognition techniques' of the type used by Mumford (1982, 1983) might be useful for the determination of ρ_E and f. Estimates of the vorticity measures ω^0 and ω^a may be obtained by 'conditional sampling techniques' as used by Townsend (1979) or by the use of multi-wire probes (such as in the work of Balint *et al.* 1986). Moreover, in numerical 'experiments' at the microscopic level based directly on the Navier–Stokes equations (such as that of Kim *et al.* 1987), it should not be difficult to calculate either $\boldsymbol{d}$ or ρ_E with the preceding discussion as guidelines.

3. Simplified equations for incompressible viscous turbulent flow

In our previous discussion of constitutive equations for turbulent flow (I, §6), our intention was chiefly to illustrate the procedure (outlined at the end of I, §5) for placing restrictions on the constitutive equations in a fairly general manner and with the aid of a few simplifying assumptions. To meet this objective, it was necessary to assume that the dependence of the Helmholtz free energy ψ and various other response functions on d_i and $d_{i,j}$ is fairly simple (i.e. linear in $d_{i,j}$ and quadratic in d_i). The purpose of the present section is to derive a relatively simple set of governing equations that incorporate most (if not all) of the basic features of turbulent fluid flow, and at the same time suppress terms which do not appear to possess clear physical significance.

Also, the functional dependence of certain response functions on d_i and $d_{i,j}$ is somewhat extended here over that assumed in I (§6) so as to account for a certain physical effect that for the sake of simplicity was neglected previously. In particular, we now assume the free energy ψ to have the form (compare with I, equation (6.14)):

$$\psi = \psi_0 + \psi_1 d_{i,i} + \psi_2 d_i d_i + \psi_3 d_{i,j} d_{i,j}. \tag{3.1}$$

It should be noted that the addition of the last term in (3.1) may be significant in some situations. Indeed, as will become apparent from our later discussions (Part II, §§5.3 and 5.4), the last term in (3.1) may be associated with certain effects caused by the extension of fairly long microscopic vortices. (Such effects are sometimes referred to as 'non-local' in the literature (Champagne *et al.* 1970, p. 83).)

The structure of the constitutive equations developed in I (§6) is at least as complex as that found in many theories of viscoelastic and other non-newtonian fluids; and, hence, a drastic simplification of these equations is clearly desirable. In proceeding with such a simplification, we are guided both by physical intuition and various experimental observations recorded in the literature, as well as by certain additional restrictions that are consistent with aspects of the Second Law of Thermodynamics. Although the theoretical developments in I are carried out for both compressible and incompressible fluids, we confine our attention in Part II to an incompressible fluid only.

In addition to the simplifying assumptions introduced previously (I, §§6 and 8, especially equations (6.12) and (8.13)), we also assume here that the dissipation of turbulence (associated with parts of the variables ξ_{H} and ξ_{T}) is unaffected by flow anisotropy, rate quantities and temperature gradients. In light of (3.1) and the preceding discussion, we now introduce constitutive equations for the determinate part of the remaining response functions as follows:

$$\left.\begin{aligned}
\hat{k}_i &= 2\rho\psi_2 d_i + \nu_1 h_i - 2\mu_6 d_j A_{ij},\\
\hat{m}_{ij} &= \rho\psi_1 \delta_{ij} + 2\rho\psi_3 d_{i,j},\\
t^*_{ij} + \tilde{t}_{ij} &= -p\delta_{ij} - \rho\psi_1 d_{j,i} - 2\rho\psi_3 d_{k,i} d_{k,j}\\
&\quad + \mu_6(d_i h_j + d_j h_i) - \mu_6 d_k(d_i A_{jk} - d_j A_{ik})\\
&\quad + 2\mu_8 A_{ij} + \tfrac{1}{2}\nu_1(d_i h_j - d_j h_i),\\
p_{\mathrm{H}i} &= -\kappa_0 g_{\mathrm{H}i}, \quad p_{\mathrm{T}i} = -\lambda_0 g_{\mathrm{T}i}, \quad \xi_{\mathrm{E}} = \gamma_0 \dot{\theta}_{\mathrm{T}},\\
\xi_{\mathrm{H}} &= \phi_0 + \frac{\kappa_0}{\rho\theta_{\mathrm{H}}} g_{\mathrm{H}i} g_{\mathrm{H}i},\\
\xi_{\mathrm{T}} &= -\frac{\theta_{\mathrm{H}}}{\theta_{\mathrm{T}}}\phi_0 + \frac{\lambda_0}{\rho\theta_{\mathrm{T}}} g_{\mathrm{T}i} g_{\mathrm{T}i} + \frac{\nu_1}{\rho\theta_{\mathrm{T}}} h_i h_i + \frac{2\mu_8}{\rho\theta_{\mathrm{T}}} A_{ij} A_{ij},\\
\epsilon &= c_{\mathrm{H}}\theta_{\mathrm{H}} + c_{\mathrm{T}}\theta_{\mathrm{T}}.
\end{aligned}\right\} \tag{3.2}$$

The coefficients ϕ_0, κ_0, λ_0, μ_8 and ν_1 in (3.2) must be non-negative and the coefficients $\psi_0 \ldots \psi_3$ in (3.1) must satisfy the three conditions in I (equations (8.17)), as well as

$$\psi_3 = \theta_{\mathrm{T}} \frac{\partial\psi_3}{\partial\theta_{\mathrm{T}}} + \gamma_0 \theta_{\mathrm{T}} \frac{\partial\psi_3}{\partial\rho_{\mathrm{E}}}. \tag{3.3}$$

The last condition (3.3) is obtained by the same procedure which led to the results in I (equations (8.17)). Also, in (3.2) p is a Lagrange multiplier due to the constraint of incompressibility introduced previously (I, equation (6.26)) and the rate-type variables h_i, A_{ij}, W_{ij} are defined in I (§5, equations $(5.1)_{3,4}$ and $(5.29)_1$).

The magnitude d of $\boldsymbol{d}$ is given by (see I, equation (5.15))

$$d = d_i a_i^3, \tag{3.4}$$

where a_i^3 are the components of the principal direction $\boldsymbol{a}^3$ of the rate of deformation tensor associated with the largest positive rate of stretching. The constitutive coefficients in (3.1) and

(3.2) are in general functions of the variables θ_H, θ_T, and ρ_E (although dependence on θ_H is often suppressed in some of these), and c_H and c_T are constant thermal and turbulent specific heats. (Possible variation of c_H with θ_H is neglected here.)

Recalling the incompressibility condition and the local conservation laws from I (equations (6.24), (5.27), (5.28), (5.3) and (4.3) and (4.4), using the constitutive expressions (3.1) and (3.2) and the simplifying assumptions (8.13) of I, after some straightforward algebraic manipulations the governing equations for incompressible viscous turbulent flow become:

$$v_{i,i} = 0, \tag{3.5}$$

$$\tfrac{1}{12}\rho d_i \dot{w}_i = \rho l_i d_i - 2\rho\psi_2 d^2 + 2\mu_6 d_i d_j A_{ij} - \nu_1 d_i h_i + \rho\psi_{1,i} d_i + 2\rho\, d_i(\psi_3 d_{i,j})_{,j}, \tag{3.6}$$

$$\begin{aligned}\rho\dot{v}_i = \rho b_i - p_{,i} + \frac{\partial}{\partial x_j}\{&\mu_6(d_i h_j + d_j h_i) + \rho d_i l_j - \tfrac{1}{12}\rho d_i \dot{w}_j + \mu_6 d_l(d_i A_{jl} + d_j A_{il}) + 2\mu_8 A_{ij} \\ &- \tfrac{1}{2}\nu_1(d_i h_j + d_j h_i) - \rho\psi_1 d_{j,i} - 2\rho\psi_3 d_{k,i} d_{k,j} - 2\rho\psi_2 d_i d_j + \rho d_i \psi_{1,j} + 2\rho d_i(\psi_3 d_{j,k})_{,k}\},\end{aligned} \tag{3.7}$$

$$\dot{\rho}_E = \gamma_0 \dot{\theta}_T, \tag{3.8}$$

$$\rho c_H \dot{\theta}_H = (k_H \theta_{H,i})_{,i} + \rho\hat{\phi}_0, \tag{3.9}$$

$$\rho c_T \dot{\theta}_T = (k_T \theta_{T,i})_{,i} - \rho\hat{\phi}_0 + \{2\rho\psi_2 d_i w_i + \rho(\psi_1 \delta_{ij} + 2\psi_3 d_{i,j})(w_{i,j} - v_{k,j} d_{i,k}) + \nu_1 h_i h_i + 2\mu_8 A_{ij} A_{ij}\}, \tag{3.10}$$

where the thermal and turbulent heat conductivities k_H and k_T and the coefficient $\hat{\phi}_0$ are defined as

$$k_H = \theta_H \kappa_0, \quad k_T = \theta_T \lambda_0, \quad \hat{\phi}_0 = \theta_H \phi_0. \tag{3.11}$$

In recording the equations of motion (3.6)–(3.9) we have already adopted the inertia coefficients (2.8) of §2 and all other quantities in (3.6) and (3.7) were defined previously in I. Also, all other coefficients in (3.6)–(3.10) are assumed to be functions of ρ_E and θ_T only. It is worth observing that various constitutive coefficients in (3.6)–(3.10) can be associated with physical processes occurring on the microscopic scale as follows:

γ_0 – rate of production of large (class 2) eddies,
k_H – diffusion of thermal heat,
k_T – diffusion of turbulent fluctuations,
$\hat{\phi}_0$ – dissipation of turbulent fluctuations,
ψ_0 – some aspect of compressibility,
$\psi_1, \psi_2, \mu_6, \nu_1$ – decay and production of flow anisotropy,
ψ_3 – nonlocal effects associated with vortex stretching,
μ_8 – production of turbulent fluctuations in the absence of vortex stretching.

The first term in (3.1), namely ψ_0, does not appear in (3.6)–(3.10), because these equations apply to an incompressible fluid only. The coefficient μ_8 must be retained so that the Navier–Stokes equations are recovered again in the absence of turbulence. We may also observe that in the absence of the director and its gradient ($d_i = d_{i,j} = 0$), but with μ_8 non-zero, the resulting equations would be similar to those of 'eddy-viscosity' type models sometimes used in the literature. We recall in this connection that μ_8 depends on ρ_E (which is related to the 'mixing length') and on θ_T (which is related to the 'turbulent kinetic energy'). Also, the various terms containing the coefficients ψ_1, ψ_2, μ_6 and ν_1 are associated with the production and decay of the macroscopic 'anisotropy' due to microscopic vortex stretching, as represented on the macroscopic scale by the director $\boldsymbol{d}$.

The terms occurring between brackets in (3.7) represent the ordinary stress tensor $\bar{t}_{ij}+\tilde{t}_{ij}$, apart from the indeterminate part arising from incompressibility, (I, equations (6.25) and (6.26)) and the terms occurring between brackets in the balance of turbulent entropy (3.10) represent the rate of production of turbulent fluctuations in the medium. Although these terms are fairly complex, it should be emphasized that their forms are not chosen by *ad hoc* assumptions here, but rather they are obtained as necessary consequences of the simpler and more intuitive assumptions related to various other effects already described in this section. Several studies found in the literature begin by introducing *ad hoc* assumptions for t_{ij} and an expression for the rate of production of 'turbulent kinetic energy', as well as assumptions for various other quantities (some of which may be regarded as analogous to those introduced in the present paper). Apart from the fact that these studies are not based on a properly formulated thermodynamical theory, the form of the correct expressions for t_{ij} and rate of turbulence production are not necessarily easily determined by just intuitive guessing.

We also note that the 'cascade' process of energy transfer from the macroscopic flow to the large turbulent eddies (through vortex stretching, etc.) and finally to the small eddies, which dissipate the energy into thermal heat, is included in, and is even an intrinsic part of, the present theory. In particular, the rate of deformation and vorticity of the macroscopic flow (as described by A_{ij} and W_{ij}, the latter of which is included in h_i) causes stretching of the large vortices and thus increases the values of d_i and w_i in (3.6). This increase, in turn, contributes to the production of turbulent fluctuations in (3.10). The increase in θ_{T} due to an increase in d_i is balanced by the dissipation of turbulence in (3.10) associated with the coefficient $\hat{\phi}_0$. This dissipation also appears as a source of thermal heat in (3.9), thus completing the cascade process.

4. Determination of the constitutive coefficients

Already in §2 we have identified the inertia coefficients y_1, y_2, which occur in the equations of motion (see I, equations $(2.10)_{2,3}$ or (5.26)–(5.28)). Our goal here is to provide estimates for certain of the constitutive coefficients in §3. Some of these estimates are based necessarily on highly idealized 'cartoons' of processes occurring on the microscopic level.

4.1. *Dissipation of turbulence*

Consider a fixed box of constant volume V containing a turbulent fluid with a constant number $V\rho_{\mathrm{E}}$ (large class 2) eddies, all of which possess equal circulation at a given time t and distance r from their central axes. Let each eddy have the same constant 'equivalent length' L and constant radius r_0 and suppose that the eddies completely span the volume V, so that

$$r_0^2 L\rho_{\mathrm{E}} = \text{const.} \tag{4.1}$$

Consider now a sequence of similar boxes for all of which the eddies have the same 'equivalent length' but differ from one another in the radius r_0. For such sequence of boxes, (4.1) implies that

$$r_0 \propto \rho_{\mathrm{E}}^{-\frac{1}{2}}. \tag{4.2}$$

The large eddies are known to pass energy down to smaller dissipating eddies through an 'inviscid' process (i.e. a process not dependent upon the microscopic viscosity μ^*). Because the large eddies contain most of the turbulent kinetic energy, the typical vorticity of one of these eddies has magnitude ω^* such that

$$\omega^* \propto u/r_0, \tag{4.3}$$

where u is the average speed of turbulent fluctuation of the large eddies within the box. Because the kinetic energy per unit mass contained within each eddy varies as $Lr_0^2 u^2$ and the turbulent temperature is proportional to the total microscopic kinetic energy of all the eddies in a given box (of constant volume V), with the help of (4.2) we find that

$$\theta_T \propto \rho_E Lr_0^2 u^2 \propto u^2. \tag{4.4}$$

Assuming that some fraction, say $\bar{f}$, of the kinetic energy of each eddy is passed down to the smaller dissipating eddies during each period of rotation, it follows from (4.3) and (4.4) that

$$d\theta_T/dt \propto -\bar{f}\theta_T\omega^* \propto \rho_E^{\frac{1}{2}}\theta_T^{\frac{3}{2}}. \tag{4.5}$$

Comparing (4.5) with the macroscopic equation (3.10) in the absence of turbulent production and diffusion, we obtain a relation for the dissipation coefficient $\hat{\phi}_0$ defined in $(3.11)_3$ as

$$\hat{\phi}_0 = c_1 \rho_E^{\frac{1}{2}}\theta_T^{\frac{3}{2}}, \tag{4.6}$$

where c_1 is a constant. With the use of (4.3) and (4.4), the differential equation (4.5) can be rewritten as

$$du^2/dt \propto u^3/r_0. \tag{4.7}$$

The form (4.7) is a standard empirical estimate for the rate of decay of turbulence (Batchelor 1952, p. 106).

4.2. *Production of eddies*

Although most of the energy dissipated in turbulence is passed from the large eddies to the smaller eddies by means of an 'inviscid' process (as discussed in §4.1), some energy is dissipated directly through viscous action by the large eddies. The amount of energy dissipated by the latter mechanism is usually small compared to that dissipated by the former mechanism, so it is commonly neglected in estimates of the rate of turbulent dissipation. We now suppose that the number density of large eddies continually adjusts itself so as to minimize the direct dissipation by the action of viscosity on the scale of the large eddies. (Similarly, we would expect the number density of small eddies to be such that the energy dissipated on the scale of small eddies (passed down from the large eddies) is a minimum.) Because of the uncertain form of the large eddies and the *ad hoc* nature of this assumption, such an approach cannot be expected to yield very accurate results; however, it may serve as a re-enforcement to strictly empirical estimates.

The velocity field at time t associated with a decaying line vortex at $t = 0$ of initial circulation Γ_0 is given by Batchelor (1967, p. 204), and is recorded here (with a slight change in notation) as

$$v_\theta^* = \frac{\Gamma_0}{2\pi r}\left\{1 - \exp\left(-\frac{r^2}{4\nu^* t}\right)\right\}, \tag{4.8}$$

where $\nu^* = \mu^*/\rho^*$ is the microscopic kinematic viscosity and v_θ^* is the circumferential component of the microscopic velocity vector $\boldsymbol{v}^*$. Using (4.2) and $(2.14)_2$ and letting

$$r_c = \sqrt{(4\nu^* t)} \tag{4.9}$$

be the cut-off radius of a combined (Rankine) vortex, the turbulent temperature θ_T associated with a volume V containing a constant number $\rho_E V$ of such vortices is proportional to the total kinetic energy contained in the box and is given by

$$\theta_T \propto \rho_E L \int_0^{r_0} r(v_\theta^*)^2 \,\mathrm{d}r \propto \rho_E L \int_0^{r_0} \frac{1}{r}\left\{1-\exp\left(-\frac{r^2}{r_c^2}\right)\right\}^2 \mathrm{d}r. \tag{4.10}$$

If $r_c \ll r_0, \theta_T$ in (4.9) can be approximated by

$$\theta_T \propto \rho_E L\{1+4\ln(r_0/r_c)\}. \tag{4.11}$$

Recalling (4.9) and differentiating (4.11) with respect to t, the rate of change of θ_T due to direct viscous dissipation (temporarily denoted by $-D$) is obtained as (because L is independent of r_0)

$$D \propto \rho_E/t. \tag{4.12}$$

Solving for t in (4.11) with the use of (4.9) and substituting the result into (4.12), we obtain

$$D \propto \rho_E \exp\left(\frac{A\theta_T}{\rho_E} - C\right), \tag{4.13}$$

where A and C are constants.

Remembering the objective of minimizing the viscous dissipation D stated at the beginning of this subsection, by differentiating (4.13) with respect to ρ_E and setting the result equal to zero we have

$$\rho_E \propto \theta_T. \tag{4.14}$$

Dividing (4.14) by θ_T, differentiating the resulting equation with respect to t and comparing with the macroscopic equation (3.8), we find that

$$\gamma_0 = \rho_E/\theta_T. \tag{4.15}$$

The variation of the turbulent temperature with time (from a suitable initial time t_0) for the flow described in §4.1 can be obtained from the differential equation (4.5) and (4.14) as

$$\theta_T \propto (t-t_0)^{-1}, \tag{4.16}$$

which is equivalent to the estimate cited by Batchelor (1952, p. 134).

Alternatively, if we return to the statements preceding (4.2) in §4.1 and now specify the 'equivalent length' L as being proportional to r_0 and again considering a sequence of similar boxes, then from arguments similar to those used previously it follows that

$$r_0 \propto \rho_E^{-\frac{1}{3}}, \quad \hat{\phi}_0 \propto \rho_E^{\frac{1}{6}}\theta_T^{\frac{3}{2}}, \tag{4.17}$$

and

$$\rho_E \propto \theta_T^{\frac{3}{2}}, \quad \gamma_0 = \frac{3}{2}\frac{\rho_E}{\theta_T}. \tag{4.18}$$

With the use of (4.17) and (4.18), the decay of turbulent temperature with time, calculated from an equation similar to (4.5), is

$$\theta_T \propto (t-t_0)^{-2}. \tag{4.19}$$

The experimental results of Comte-Bellot & Corrsin (1966) and of Gad-el-hak & Corrsin (1973) indicate (after a reinterpretation of their 'root mean square' velocity data) that for the flow considered here the turbulent temperature is proportional to $(t-t_0)$ according to

$$\theta_T \propto (t-t_0)^{-\frac{4}{3}}. \tag{4.20}$$

The result (4.20) clearly falls between the estimates (4.16) and (4.19), thus indicating that the dependence of vortex 'length' L on vortex 'width' r_0 is intermediate to the two extremes considered here.

4.3. *Diffusion of thermal heat and turbulent fluctuations*

Once more we recall the flow described in §4.1, but now admit the gradients in thermal and turbulent temperatures in the x_1-direction. In particular, we consider two neighbouring eddies with equal radii r_0 and positioned such that a line running through their centres and normal to their axes is parallel to the base vector $\boldsymbol{e}_1$. With the use of formulae of the type (4.3) and the notations u_1, u_2 for average speeds of the two eddies, the central vorticities of the eddies have the magnitudes $\omega_1^* \propto u_1/r_0$ and $\omega_2^* = u_2/r_0$. The microscopic kinetic energies of the eddies per unit mass are $K_1 \propto Lu_1^2 r_0^2$ and $K_2 \propto Lu_2^2 r_0^2$, and θ_1^* and θ_2^* denote the average microscopic temperatures of the eddies. The total energy per unit mass E_1 and E_2 of the two eddies are:

$$E_1 \propto (u_1^2 + c^*\theta_1^*)\, r_0^2 L, \quad E_2 \propto (u_2^2 + c^*\theta_2^*)\, r_0^2 L, \tag{4.21}$$

where c^* is the microscopic specific heat. We now set

$$u_1 = u, \quad u_2 = u+\Delta u, \quad K_1 = K, \quad K_2 = K+\Delta K, \quad \theta_1^* = \theta^*, \quad \theta_2^* = \theta^* + \Delta\theta^*, \tag{4.22}$$

where the difference terms Δu, ΔK, $\Delta\theta^*$ in (4.22) are assumed to be small. On the assumption that during each period of eddy rotation some fraction, say $\hat{f}$, of the energy difference ΔE between the eddies is exchanged, to leading order in the 'difference' quantities the rate of energy transfer Q between the two eddies can be estimated by using (4.22) as

$$Q \propto \hat{f}(\Delta E)\, \overline{\omega^*} \sim \hat{f} u r_0 (\Delta u^2 + c^*\, \Delta\theta^*)\, L, \tag{4.23}$$

where $\overline{\omega^*}$ denotes the average value of ω_1^* and ω_2^*.

Imagine again a cubic box of volume V containing $V\rho_E$ eddies of radius r_0 and 'equivalent length' $L \gg r_0$. Then, any cross section of the box with area $A = V^{\frac{2}{3}}$ should intersect approximately either $A/r_0 L$ eddies (if axes lie parallel to the surface) or A/r_0^2 eddies (if the axes of the eddies lie perpendicular to the surface). If we recall (4.2) and the assumption that L is a constant independent of r_0, the number of eddies intersected by the cross section of the box is proportional (apart from the factor A) to either $\rho_E^{\frac{1}{2}}$ or ρ_E, which represent the extreme values. We now assume that the number of eddies intersected by the cross-sectional surface is proportional to the geometric mean of the above two estimates, namely $\rho_E^{\frac{3}{4}}$ eddies. If q is the macroscopic total heat flux (both thermal and turbulent) measured per unit area and per unit time in the $\boldsymbol{e}_1$ direction, it follows that

$$q \propto \rho_E^{\frac{3}{4}}\, Q. \tag{4.24}$$

We can further identify the thermal and turbulent temperature gradients as

$$\frac{\partial\theta_H}{\partial x} \propto \frac{\Delta\theta^*}{r_0}, \quad \frac{\partial\theta_T}{\partial x} \propto \frac{\Delta u^2}{r_0}. \tag{4.25}$$

From (4.20)–(4.22) and using (4.2), we find that

$$q = q_{\mathrm{H}} + q_{\mathrm{T}} = \rho_{\mathrm{E}}^{-\frac{1}{4}} \theta_{\mathrm{T}}^{\frac{1}{2}} \left(c_2 \frac{\partial \theta_{\mathrm{H}}}{\partial x} + c_3 \frac{\partial \theta_{\mathrm{T}}}{\partial x} \right), \tag{4.26}$$

where c_2 and c_3 are constants. The result (4.26) in conjunction with (3.9)–(3.11) implies that the thermal and turbulent heat conductivities are given by†

$$k_{\mathrm{H}} = c_2 \rho_{\mathrm{E}}^{-\frac{1}{4}} \theta_{\mathrm{T}}^{\frac{1}{2}}, \quad k_{\mathrm{T}} = c_3 \rho_{\mathrm{E}}^{-\frac{1}{4}} \theta_{\mathrm{T}}^{\frac{1}{2}}. \tag{4.27}$$

In line with the discussion preceding (4.24), the exponent attached to ρ_{E} in (4.27) may vary from $-\frac{1}{2}$ to 0 depending upon the orientation of the eddies. However, the expressions $(4.27)_{1,2}$ are consistent with the observation that diffusion rates both decrease as the number density of eddies increases at a constant θ_{T} and also increase as θ_{T} increases at a constant ρ_{E}.

Alternatively, rather than assuming that L is a constant, we may assume that it is proportional to r_0. If this is adopted, an argument similar to that given above yields the results.

$$Q \propto r_0^3 \theta_{\mathrm{T}}^{\frac{1}{2}} \left(\frac{\Delta u^2}{r_0} + \frac{c^* \Delta\theta^*)}{r_0} \right), \quad q \propto \rho_{\mathrm{E}}^{\frac{2}{3}} Q,$$

so that

$$k_{\mathrm{H}} \propto \rho_{\mathrm{E}}^{-\frac{1}{3}} \theta_{\mathrm{T}}^{\frac{1}{2}}, \quad k_{\mathrm{T}} \propto \rho_{\mathrm{E}}^{-\frac{1}{3}} \theta_{\mathrm{T}}^{\frac{1}{2}}. \tag{4.28}$$

4.4. *Coefficients in the expression for free energy*

The coefficients in the expression for the free energy ψ, namely ψ_1, ψ_2 and ψ_3, are restricted to satisfy the equations (3.3) and the two equations in Part I (equations $(8.17)_{2,3}$). These restrictions result as a consequence of the assumption $(3.2)_9$ for ϵ in conjunction with the more general thermodynamical restrictions obtained in I (§6). Assuming that the coefficient γ_0, which occurs in the expression $(3.2)_6$ for ξ_{E}, is of the form

$$\gamma_0 = c(\rho_{\mathrm{E}}/\theta_{\mathrm{T}}), \tag{4.29}$$

where c is a constant, then one possible form for the coefficients ψ_n $(n = 1, 2, 3)$ that satisfies the above restriction identically is

$$\psi_n = c_{n+3} \theta_{\mathrm{T}}^m \rho_{\mathrm{E}}^{(1-m)/c} \quad (n = 1, 2, 3), \tag{4.30}$$

where c_4, c_5, c_6 and m are arbitrary constants. In particular, if we assume that a change in ρ_{E} does not affect the free energy ψ, then we can set m equal to one in (4.30) and obtain

$$\psi_1 = c_4 \theta_{\mathrm{T}}, \quad \psi_2 = c_5 \theta_{\mathrm{T}}, \quad \psi_3 = c_6 \theta_{\mathrm{T}}. \tag{4.31}$$

The simple results (4.31) appear to be reasonable and at the same time are consistent with previous developments. If necessary, however, we could accommodate alternative forms in accordance with (4.30) when $m \neq 1$.

4.5. *Viscosity coefficients*

So far we have not been able to devise simple and convincing arguments to determine the functional forms of the viscosity coefficients μ_6, μ_8 and ν_1 (similar to the arguments presented

† In writing $(4.27)_1$ it is implicitly assumed that the contribution to k_{H} by the microscopic heat conductivity k^* is negligible.

previously in this section). It may be recalled, however, that in the usual 'mixing length' approximation the 'turbulent viscosity' $\nu_T(=\mu_T/\rho)$ is assumed to vary as

$$\nu_T \propto u r_0, \tag{4.32}$$

where u is the average fluctuation speed introduced earlier in (4.3) and r_0 is a typical width (i.e. the 'mixing length') of the eddies (see Tennekes & Lumley 1972, p. 44, equation (2.3.9)). From (4.2) and (4.4), we know that $u \propto \theta_T^{\frac{1}{2}}$ and $r_0 \propto \rho_E^{-\frac{1}{2}}$, so that after identification of the type $(\mu_8/\rho) = \nu^* + \nu_T$ (4.32) implies

$$\mu_8 = c_7 \rho \theta_T^{\frac{1}{2}} \rho_E^{-\frac{1}{2}} + \mu^*, \tag{4.33}$$

where c_7 is a positive constant and μ^* is the microscopic viscosity. In obtaining (4.33), it is observed that μ_8/ρ plays the same role as the usual 'turbulent viscosity' ν_T (after neglecting μ^* in (4.33), of course). Alternatively, if we assume that the vortex 'length' L is proportional to r_0, the exponent of ρ_E in (4.33) becomes $-\frac{1}{3}$ rather than $-\frac{1}{2}$.

5. Solutions of some simple turbulent flow problems

In this section, we consider the solution of the macroscopic equations of §3 for certain specific anisotropic turbulent flows, for the purpose of illustrating the use of these equations in solving turbulent boundary and initial value problems. We first consider the conditions under which a constant uniform gradient in the velocity $\boldsymbol{v}$ can exist throughout the flow, including the special case in which this gradient vanishes. The results of this discussion are then applied to study the gradual return to 'isotropy' of an initially 'anisotropic' fluid when the gradient in the velocity $\boldsymbol{v}$ is vanishingly small. Alternative simplification of the equations of §3 appropriate to plane turbulent channel flow is next considered, and this is followed by a detailed comparison of the theoretical predictions for plane turbulent Poiseuille flow with the experimental results of Laufer (1951).

5.1. *Flow possessing a constant uniform velocity gradient*

Perhaps the simplest type of turbulent shear flow to study analytically is flow possessing a constant uniform gradient in the ordinary velocity $\boldsymbol{v}$. Such flows are sometimes referred to in the literature as a special case of the class of 'homogeneous' turbulent flows (see Champagne *et al.* 1970). We consider, in particular, the possibility of a flow in which the velocity has the form

$$\boldsymbol{v} = (Ax_2 + B)\,\boldsymbol{e}_1, \tag{5.1}$$

where A and B are constants, and in which all other variables are independent of x_2 and x_3. Assuming that the constant A is positive and recalling equation $(5.10)_1$ of Part I, the direction $\boldsymbol{a}^3$ along which the director is aligned can be easily calculated to be

$$a_i^3 = [\tfrac{\surd 2}{2}, \tfrac{\surd 2}{2}, 0], \tag{5.2}$$

so that $d_1 = d_2 = \frac{\surd 2}{2} d$ and $d_3 = 0$. If we take $\boldsymbol{b} = \boldsymbol{l} = \boldsymbol{0}$ and denote by w the magnitude of the director velocity $\boldsymbol{w}$, the equations of motion (3.6) and (3.7) for such a flow are given by

$$\tfrac{1}{12}\rho \dot{w} = -2\rho\psi_2 d + \mu_6 A d - \nu_1 w + \tfrac{\surd 2}{2}\rho \frac{\partial \psi_1}{\partial x} + 2\rho \frac{\partial}{\partial x}\left(\psi_3 \frac{\partial d}{\partial x}\right), \tag{5.3}$$

$$p = p_0 + \left\{ (\mu_6 - \tfrac{1}{2}\nu_1)\, wd - \tfrac{1}{24}\rho\dot{w}d - \tfrac{\sqrt{2}}{2}\rho\psi_1 \frac{\partial d}{\partial x} - 2\rho\psi_3 \left(\frac{\partial d}{\partial x}\right)^2 - \rho\psi_2 d^2 + \tfrac{\sqrt{2}}{2}\rho d \frac{\partial \psi}{\partial x} + \rho d \frac{\partial}{\partial x}\left(\psi_3 \frac{\partial d}{\partial x}\right) + \tfrac{1}{4}\nu_1 A d^2 \right\}, \quad (5.4)$$

$$\frac{\partial}{\partial x}\left\{ (\mu_6 - \tfrac{1}{2}\nu_1)\, wd - \tfrac{1}{24}\rho\dot{w}d + \tfrac{1}{2}\mu_6 A d^2 + \mu_8 A - \rho\psi_2 d^2 + \tfrac{\sqrt{2}}{2}\rho d \frac{\partial \psi_1}{\partial x} + \rho d \frac{\partial}{\partial x}\left(\psi_3 \frac{\partial d}{\partial x}\right)\right\} = 0, \quad (5.5)$$

where p_0 is a constant of integration.

Using (5.3), we can reduce (5.5) to the simpler form

$$\frac{\partial}{\partial x}\left\{ \mu_6 wd + \mu_8 A + \tfrac{\sqrt{2}}{4}\rho d \frac{\partial \psi_1}{\partial x}\right\} = 0. \quad (5.6)$$

The values of p and d are determined from (5.3) and (5.4) and ρ_E, θ_H and θ_T are determined from (3.8)–(3.10); however, because the velocity v is prescribed by (5.1), (5.6) gives an additional equation which must be satisfied identically for the assumption (5.1) to be admissible.

Although there are certain special cases in which the values of the independent variables are such that (5.6) is satisfied identically, this will not in general be the case. We must, therefore, conclude that the linear velocity profile (5.1) does not represent a general solution of the equations (3.5)–(3.10) governing the macroscopic motion of turbulent flow. This result is hardly surprising considering that a similar observation can be made even for a laminar flow where the viscosity varies with temperature and density (as is evident from (5.6) in the absence of turbulence). Several analytical and numerical studies in the literature commence with the assumption (5.1) for the ordinary velocity (see, for instance, the recent numerical work of Rogers & Moin 1987). In the light of the observation just made, the results of these studies must be viewed with some scepticism. It should perhaps also be noted that (5.6) is not necessarily satisfied even for a uniform velocity flow ($A = 0$) unless the other independent variables are also uniform in x or unless the director magnitude d vanishes. In many experimental studies, the spacial variation of ρ_E, θ_T and d is sufficiently small that the macroscopic velocity $\boldsymbol{v}$ is observed to be nearly uniform. For such a case, as will be discussed in §5.2, the velocity gradient is said to be 'vanishingly small' and may be allowed to approach zero in order to obtain approximate solutions of the given problem.

5.2. *Decay of 'anisotropy' with vanishingly small velocity gradient*

A macroscopic fluid particle that initially possesses certain directional dependence (or is 'anisotropic') with $\boldsymbol{d}$ non-zero would be expected to make a slow transition to an 'isotropic' state (in which $\boldsymbol{d}$ vanishes) when placed in a stream with vanishingly small velocity gradient grad $\boldsymbol{v}$. Various attempts to study this process experimentally have been made by Townsend (1954), Uberoi (1956), Comte-Bellot & Corrsin (1966) and Tucker & Reynolds (1968), although in the present context the data provided by these studies must be viewed as somewhat incomplete: these experimental studies are incomplete both because the range of measurements are rather limited and because they do not clearly provide data relating to the relevant physical aspects of the microscopic flow which would facilitate estimates of ρ_E and d of the present theory.

In these experiments, an incompressible fluid is first distorted (and hence made 'anisotropic') by a grid or duct of rapidly changing cross section, and then it is passed into a straight channel of constant cross-sectional area in which grad $\boldsymbol{v}$ is observed to be nearly zero. While the flow is being distorted, some of the large eddies become aligned and the diagonal components of the stress tensor t_{ij} are observed to differ from one another considerably (this giving evidence that the flow is anisotropic). When the velocity gradient vanishes in the straight uniform channel, both the alignment of large eddies and the flow anisotropy are observed to lessen very gradually.

In the absence of a velocity gradient, we would not expect the direction of alignment of the large eddies, represented by some fixed unit vector $\boldsymbol{a}$ say, to change. We therefore set

$$\boldsymbol{d} = d\boldsymbol{a}, \tag{5.7}$$

where $\boldsymbol{a}$ is determined from the initial conditions. For the purposes of this example, we assume that the external director body force $\boldsymbol{l}$ vanishes. For a steady state flow in the $x(=x_1)$ direction in which also all quantities are independent of x_2, x_3 coordinates, with the help of (5.7) the system of equation (3.6)–(3.8) and (3.10) can be reduced to

$$\left.\begin{aligned} \tfrac{1}{12}\rho v^2 \frac{\partial^2 d}{\partial x^2} &= -2\rho\psi_2 d + \rho\frac{\partial \psi_1}{\partial x}\boldsymbol{a}\cdot\boldsymbol{e}_1 + 2\rho\frac{\partial}{\partial x}\left(\psi_3\frac{\partial d}{\partial x}\right) - \nu_1 v\frac{\partial d}{\partial x},\\ \frac{\partial \rho_{\mathrm{E}}}{\partial x} &= \gamma_0\frac{\partial \theta_{\mathrm{T}}}{\partial x},\\ \rho c_{\mathrm{T}} v\frac{\partial \theta_{\mathrm{T}}}{\partial x} &= -\rho\hat{\phi}_0 + \frac{\partial}{\partial x}\left(k_{\mathrm{T}}\frac{\partial \theta_{\mathrm{T}}}{\partial x}\right) + \left\{2\rho\psi_2 v d\frac{\partial d}{\partial x} + \nu_1 v^2\left(\frac{\partial d}{\partial x}\right)^2 + \rho\left(\psi_1\boldsymbol{a}\cdot\boldsymbol{e}_1 + 2\psi_3\frac{\partial d}{\partial x}\right)v\frac{\partial^2 d}{\partial x^2}\right\}.\end{aligned}\right\} \tag{5.8}$$

If we neglect diffusion and production of turbulent fluctuations in (5.8) and assume the forms (4.6) and (4.15) for $\hat{\phi}_0$ and γ_0, we can integrate $(5.8)_{2,3}$ to obtain

$$\rho_{\mathrm{E}} = A\theta_{\mathrm{T}}, \quad \theta_{\mathrm{T}} = \left(\frac{c_1 A^{\frac{1}{2}}}{c_{\mathrm{T}} v}x + B\right)^{-1}, \tag{5.9}$$

where A and B in (5.9) are arbitrary constants of integration that can be obtained from the initial conditions on ρ_{E} and θ_{T}. Also, v is prescribed and c_1 is a constitutive constant related to the dissipation rate $\hat{\phi}_0$. Equations (5.9) imply that ρ_{E} and θ_{T} approach zero as x becomes large, as might be expected. A general solution of $(5.2)_1$ is not easily obtainable and we begin by examining a solution of $(5.2)_1$ for which ρ_{E} and θ_{T} are taken to be constants. In this case, $(5.8)_1$ reduces to

$$\tfrac{1}{12}\rho(v^2 - 24\psi_3)\frac{\partial^2 d}{\partial x^2} + \nu_1 v\frac{\partial d}{\partial x} + 2\rho\psi_2 d = 0 \tag{5.10}$$

and has a solution of the form

$$d = C\mathrm{e}^{-\beta x}, \tag{5.11}$$

where C is a constant and the temporary notion β is defined by

$$\beta = \frac{\nu_1 v \pm [\nu_1^2 v^2 - \frac{2}{3}\rho^2\psi_2(v^2 - 24\psi_3)]^{\frac{1}{2}}}{\frac{1}{6}\rho(v^2 - 24\psi_3)}. \tag{5.12}$$

Because we expect d to decrease in the downstream direction, the $\pm$ sign in (5.12) is chosen so that β is positive. It is clear from (5.12) that the term involving ν_1, and possibly also terms

PHILOSOPHICAL TRANSACTIONS OF THE ROYAL SOCIETY A MATHEMATICAL, PHYSICAL & ENGINEERING SCIENCES

involving ψ_2 and ψ_3 control the decay of flow anisotropy in the absence of a gradient in the velocity $\boldsymbol{v}$.

The solution (5.11) is compatible with previous experimental studies; however, a direct comparison of the experimental results with the solutions obtained here is not possible because the existing reported experimental studies do not provide sufficient data from which estimates for ρ_E and d can be obtained.

5.3. *Plane turbulent channel flows*

We now consider simplifications of the viscous flow equations of §3 appropriate for fully developed plane turbulent channel flows (such as plane Couette or Poiseuille flow), for which we may assume that

$$\boldsymbol{v} = v(x_2)\,\boldsymbol{e}_1. \tag{5.13}$$

Here $\boldsymbol{e}_1$ is the direction along the centreline of the channel and $\boldsymbol{e}_2$ is the direction normal to the walls of the channel, as illustrated in figure 1 for plane Poiseuille flow. From (5.13), the direction of $\boldsymbol{d}$ (i.e. $\boldsymbol{a}^3$) is found to be constant and uniform everywhere in the flow apart from a possible discontinuity corresponding to a change in the sign of grad v. Remembering that the components of $\boldsymbol{a}^3$ are calculated from grad $\boldsymbol{v}$ using (5.13), the components of $\boldsymbol{d}$ are:

$$d_i = d(\pm\tfrac{\sqrt{2}}{2}, \tfrac{\sqrt{2}}{2}, 0), \tag{5.14}$$

where the $\pm$ sign in (5.14) is chosen to correspond with the (plus or minus) sign of $\partial v/\partial x_2$.

For a fully developed plane channel flow, we would expect all variables pertaining to the macroscopic flow and the turbulent fluctuations to be functions of x_2 only. Then, (3.5) and (3.8) are satisfied identically and after calculating h_i and A_{ij} with the help of (5.13) and (5.14), setting $\boldsymbol{b} = \boldsymbol{l} = \boldsymbol{0}$ and assuming also that $\partial v/\partial x_2 > 0$, (3.6), $(3.7)_{1,2}$ and (3.10) become

$$\frac{\partial}{\partial x_2}\left(\psi_3\frac{\partial d}{\partial x_2}\right) + \left(\frac{\mu_6}{2\rho}\frac{\partial v}{\partial x_2} - \psi_2\right)d + \tfrac{\sqrt{2}}{4}\frac{\partial \psi_1}{\partial x_2} = 0, \tag{5.15}$$

$$\frac{\partial}{\partial x_2}\left\{(\tfrac{1}{2}\mu_6 d^2 + \mu_8)\frac{\partial v}{\partial x_2} - \rho\psi_2 d^2 + \tfrac{\sqrt{2}}{2}\rho d\frac{\partial \psi_1}{\partial x_2} + \rho d\frac{\partial}{\partial x_2}\left(\psi_3\frac{\partial d}{\partial x_2}\right)\right\} = \frac{\partial p}{\partial x_1}, \tag{5.16}$$

$$p = p_0(x_1) + \left\{(\mu_6 - \tfrac{1}{4}\nu_1)\,d^2\frac{\partial v}{\partial x_2} - \tfrac{\sqrt{2}}{2}\rho\left(\psi_1\frac{\partial d}{\partial x_2} - d\frac{\partial \psi_1}{\partial x_2}\right)\right.$$
$$\left. - \rho\psi_2 d^2 - 2\rho\psi_3\left(\frac{\partial d}{\partial x_2}\right)^2 + \rho d\frac{\partial}{\partial x_2}\left(\psi_3\frac{\partial d}{\partial x_2}\right)\right\}, \tag{5.17}$$

$$\rho\hat{\phi}_0 = \frac{\partial}{\partial x_2}\left(k_T\frac{\partial \theta_T}{\partial x_2}\right) + (\tfrac{1}{4}\nu_1 d^2 + \mu_8)\left(\frac{\partial v}{\partial x_2}\right)^2. \tag{5.18}$$

The results (5.15)–(5.18) provide a sufficient number of equations for the determination of d, v, p and θ_T as functions of x_2. Using (5.15) and integrating once with respect to x_2, (5.16) becomes

$$\mu_8\frac{\partial v}{\partial x_2} + \tfrac{\sqrt{2}}{4}\rho d\frac{\partial \psi_1}{\partial x_2} = x_2\frac{\partial p_0}{\partial x_1} + A, \tag{5.19}$$

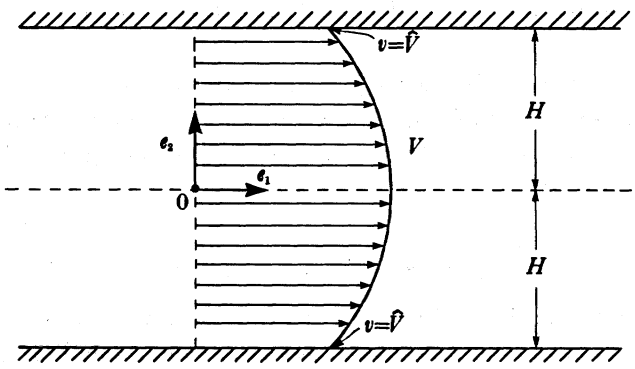

FIGURE 1. A sketch of two-dimensional Poiseuille flow in x_1–x_2 plane of width $2H$ showing the velocity profile with $\hat{V}$ as the wall velocity.

where A is another constant of integration and p_0 is a prescribed function of x_1. Assuming that ψ_1 and d are known, (5.19) yields a solution for $\partial v/\partial x_2$. Elimination of $\partial v/\partial x_2$ between (5.15) and (5.19) results in the following differential equation for d:

$$0 = \frac{\partial}{\partial x_2}\left(\psi_3 \frac{\partial d}{\partial x_2}\right) + \left[\frac{\mu_6}{2\rho\mu_8}\left(A + x_2 \frac{\partial p_0}{\partial x_1}\right) - \psi_2\right] d - \tfrac{\sqrt{2}}{8}\frac{\mu_6}{\mu_8} d^2 \frac{\partial \psi_1}{\partial x_2} + \tfrac{\sqrt{2}}{4}\frac{\partial \psi_1}{\partial x_2}. \tag{5.20}$$

Using (5.19) and the estimates (4.8) and $(4.29)_2$ for $\hat{\phi}_0$ and k_{T}, where ρ_{E} is assumed to be a known function of x_2, (5.18) yields an equation for θ_{T} of the form

$$\rho c_1 \rho_{\mathrm{E}}^{\frac{1}{2}} \theta_{\mathrm{T}}^{\frac{3}{2}} = \frac{\partial}{\partial x_2}\left(c_3 \rho_{\mathrm{E}}^{-\frac{1}{4}} \theta_{\mathrm{T}}^{\frac{1}{2}} \frac{\partial \theta_{\mathrm{T}}}{\partial x_2}\right) + \frac{1}{\mu_8}\left(\frac{1}{4}\frac{\nu_1}{\mu_8} d^2 + 1\right)\left(A + x_2 \frac{\partial p_0}{\partial x_1} - \tfrac{\sqrt{2}}{4}\rho d \frac{\partial \psi_1}{\partial x_2}\right)^2. \tag{5.21}$$

It should be emphasized that because the coefficients of ψ in (5.20) depend on θ_{T} and because d appears explicitly in (5.19) and (5.21), these equations for $\partial v/\partial x_2$, d and θ_{T} are coupled.

As discussed in I (§3), constitutive equations must also be found for the various supply terms in the jump conditions at the walls as functions of the values of the various independent variables evaluated at the walls, as well as certain intrinsic features of the walls (such as surface roughness). The slip velocities $V_2 - \hat{V}_2$ and $V_1 - \hat{V}_1$, where V_1, V_2 are the velocities of the walls and $\hat{V}_1$, $\hat{V}_2$ are the velocities of the fluid bordering these walls, as well as various boundary conditions for the other independent variables such as ρ_{E}, θ_{T} and d, may be obtained from the jump conditions appropriate to turbulent-nonturbulent interfaces (as presented in I, §7) once the forms of the surface supply terms appearing in these jump conditions are known.

Finally, we note that if ψ_3 is set to zero in (5.20), we are left with a simple quadratic equation for d. In this case, no independent boundary conditions can be required for d, so that production of d along the boundaries will not directly affect the value of d within the body of the flow. Recalling the terminologies of §2.1, we note that since the eddy lengths may become comparable to the size of the microscopic region $\mathscr{P}'$ associated with a macroscopic point $\boldsymbol{x}$, it seems reasonable that the intensity of vortex stretching in a given fluid element might affect the level of vortex stretching in its neighbouring fluid elements. For this reason, it is advantageous to admit non-zero values of ψ_3 (which is related to the 'non-local' effect discussed above) in a general theory of turbulent channel flow. However, in certain regions of the flow and for the idealized case of extremely high-intensity turbulence (for large θ_T), where this effect may be neglected, we set ψ_3 equal to zero in (5.20) to obtain a solution for d in the form

$$d\frac{\partial\psi_1}{\partial x_2} = \left[\frac{\sqrt{2}}{\rho}\left(A + x_2\frac{\partial p_0}{\partial x_1}\right) - 2\sqrt{2}\frac{\psi_2\mu_8}{\mu_6}\right] \pm \left\{\left[\frac{\sqrt{2}}{\rho}\left(A + x_2\frac{p_0}{\partial x_1}\right) - 2\sqrt{2}\frac{\psi_2\mu_8}{\mu_6}\right]^2 + \frac{2\mu_8}{\mu_6}\left(\frac{\partial\psi_1}{\partial x_2}\right)^2\right\}^{\frac{1}{2}}. \tag{5.22}$$

At this point, it may be enlightening to compare the present theory with the usual 'Reynolds stress' formulation of turbulence. We note that for plane channel flows, the macroscopic velocity $\boldsymbol{v}$ of the present theory and the usual 'mean' velocity become identical (because $\boldsymbol{w}$ vanishes in (2.9)). The 'mean' momentum equation for incompressible turbulent channel flow is (see Reynolds 1976, equation (2.1a))

$$\frac{\partial\overline{p^*}}{\partial x} = \mu^*\frac{\partial^2 v}{\partial y^2} - \rho\frac{\partial R_{12}}{\partial y}, \tag{5.23}$$

where $\overline{p^*}$ is the averaged pressure, μ^* is the dynamic viscosity of the fluid, $v = \boldsymbol{v}\cdot\boldsymbol{e}_1$ is the 'mean' (or the macroscopic) velocity in the $\boldsymbol{e}_1$-direction and R_{12} is the relevant component of the 'Reynolds stress' tensor. Comparing (5.23) with (5.16) and after identifying $(x_1, x_2) = (x, y)$, $\overline{p^*}$ with p and assuming the form (4.33) for μ_8, the component R_{12} of the Reynolds stress is readily identified as

$$\rho R_{12} = (\tfrac{1}{2}\mu_6 d^2 + c_7\rho\theta_T^{\frac{1}{2}}\rho_E^{-\frac{1}{3}})\frac{\partial v}{\partial y} - \rho\psi_2 d^2 + \tfrac{\sqrt{2}}{2}\rho d\frac{\partial\psi_1}{\partial y} + \rho d\frac{\partial}{\partial y}\left(\psi_3\frac{\partial d}{\partial y}\right). \tag{5.24}$$

The coefficients on the right-hand side of (5.24) are functions of ρ_E and θ_T only. The value of d at the wall of the channel (which influences the value of R_{12} in (5.24) at the wall) is strongly influenced by both the slip velocity along the wall and the macroscopic velocity gradient. The result (5.24) indicates that both the macroscopic velocity gradient and the wall slip velocity contribute to the stress acting on the wall. In fact, the expression (5.24) may be interpreted (in the special context of channel flow) as a constitutive equation for R_{12}.

5.4. *Solution for turbulent plane Poiseuille flow in a two-dimensional channel*

It is now of interest to consider a detailed comparison of the predictions of the theory for the channel flow equations obtained in §5.3 with a relevant experimental study. For this purpose, we consider a plane Poiseuille flow, as illustrated in figure 1, and compare our solution with the experimental results of Laufer (1951). (The results of §5.3 are also applicable to plane Couette flow; however, the available experimental data are not as detailed for this problem.)

The equations applicable to a plane turbulent Poiseuille flow are given by (5.19)–(5.21) with $A = 0$, where the simplification (5.22) may be used in place of (5.20) under certain circumstances. Because these equations are coupled and highly nonlinear, an exact analytical solution (in the context of the present theory) for this flow is not readily attainable. Furthermore, because there still remains several constants in some of the constitutive equations that have not yet been identified, a full numerical solution for this problem is not possible at this time and even with some guesses at the values of the constants, may not be particularly enlightening. For these reasons, and partially in response to suggestions made by Laufer (1951, 1954), the flow field is divided up into three regions, and a simplistic approximate solution is obtained in each of the three regions. Comparison with the data of Laufer (1951) then allows one to make estimates for certain of the as yet undermined response constants and to verify that solutions which are compatible with the experimental findings are predicted by the present theory.

Both the solutions presented here and the experiment of Laufer (1951) are relevant to air flow through a 12.7 cm wide channel at a Reynolds number of 61600 (based upon the maximum value of v and one half the channel width of 2H), and streamwise pressure gradient of $\partial p/\partial x_1 = -5.67$ kg s^{-2} m^{-2}. Based on Laufer's 'turbulent microscale' measurements, a rough estimate for eddy density (assumed constant across the channel width) is calculated to be $\rho_E \approx 6.4$ eddies per cubic centimetre. Using (2.13) and (2.14), the value of turbulent temperature θ_T is obtained from Laufer's measurements of root-mean-square values of the (microscopic) velocity fluctuations and is plotted in figure 2. Also, since the director velocity $\boldsymbol{w}$ vanishes identically for this flow, the macroscopic velocity $\boldsymbol{v}$ and Laufer's 'mean' velocity are identical. Finally, the constitutive coefficients $\hat{\phi}_0$, k_T, ψ_1, ψ_2, ψ_3 and μ_8 are assumed to be given by (4.6), $(4.27)_2$, $(4.31)_{1,2,3}$ and (4.33), respectively, and the remaining coefficients μ_6 and ν_1 are simply assumed to be constants.

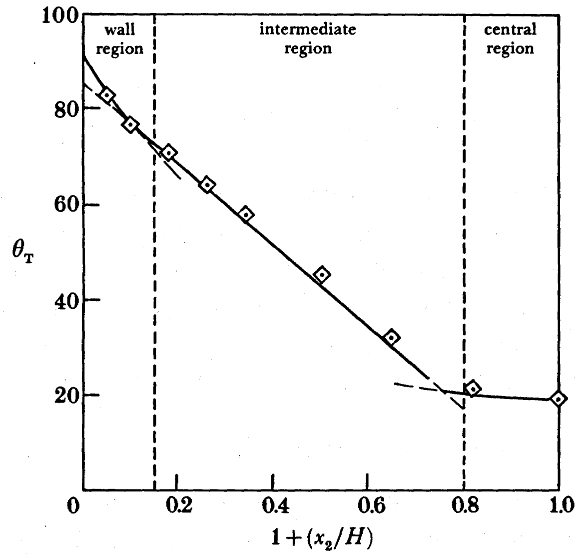

FIGURE 2. Variation of turbulent temperature θ_T along the half-width of the channel $(-H \leqslant x_2 \leqslant 0)$ plotted against $1+(x_2/H)$, as predicted by the present theory (solid lines) and its comparison with experimental measurements (◇) of Laufer (1951). The theoretical predictions are calculated from equations (5.25), (5.27), (5.30) and the experimental points represent the converted form of data given in figs 11, 13, 14 of Laufer (see also the discussion under Results in §5.4).

(i) *Solution in central region* $(0.8 \leqslant 1+(x_2/H) \leqslant 1)$

The measurements of Laufer (1951, p. 1264, fig. 27) indicate that in the region containing the centre part of the flow (defined above) the diffusion and dissipation of turbulent fluctuations are nearly balanced and the production of turbulence is negligible. If we thus neglect the production term in (5.21), we are left with

$$\rho c_1 \rho_E^{\frac{1}{3}} \theta_T^{\frac{3}{2}} = \frac{\partial}{\partial x_2}\left(c_3 \rho_E^{-\frac{1}{4}} \theta_T^{\frac{1}{2}} \frac{\partial \theta_T}{\partial x_2}\right). \tag{5.25}$$

Neglecting also quadratic terms in the derivative $\partial\theta_T/\partial x_2$, (5.25) can be rearranged as

$$\frac{\partial^2\theta_T}{\partial x_2^2} = \frac{\rho c_1 \rho_E^{\frac{3}{2}}}{c_3}\theta_T. \tag{5.26}$$

Given that c_1 and c_3 are non-negative and that the temperature gradient $\partial\theta_T/\partial x_2$ is zero along the centreline $x_2 = 0$, a solution of (5.26) is

$$\theta_T = B\exp\left[\left(\frac{\rho c_1 \rho_E^{\frac{3}{2}}}{c_3}\right)^{\frac{1}{2}} x_2\right] + B\exp\left[-\left(\frac{\rho c_1 \rho_E^{\frac{3}{2}}}{c_3}\right)^{\frac{1}{2}} x_2\right], \tag{5.27}$$

where B is a constant of integration.

(ii) *Intermediate region* $(0.15 \leqslant 1+(x_2/H) \leqslant 0.8)$

In the intermediate region (defined above), the production of turbulence becomes a major contributor to the turbulent temperature equation (5.21). It is convenient for our present purpose and consistent with the later observations of Laufer (1954) to assume that in this intermediate region the production and dissipation of turbulence are completely balanced and the effect of diffusion is negligible. Indeed, such an approximation enables us to obtain a compact analytical expression for θ_T. If the contribution to the production of turbulence by the director is also neglected in this region, (5.21) reduces simply to

$$\rho c_1 \rho_E^{\frac{1}{2}} \theta_T^{\frac{3}{2}} = \frac{x_2^2}{\mu_8}\left(\frac{\partial p_0}{\partial x_1}\right)^2. \tag{5.28}$$

Substituting the expression (4.33) for μ_8 (after neglecting the term involving μ^*) into (5.28), and taking the square root of the resulting equation, we obtain a solution for θ_T as

$$\theta_T = \frac{1}{\rho}\frac{x_2}{\sqrt{(c_1 c_7)}}\frac{\partial p_0}{\partial x_1}. \tag{5.29}$$

(iii) *Wall region* $(0 \leqslant 1+(x_2/H) \leqslant 0.15)$

Near the wall, we would expect the influence of the director on both θ_T and v to become fairly large, as is evidenced indirectly by the rapid changes in v and θ_T with x_2 in this region. An estimation of Laufer's (1951) data for θ_T and v suggests further simplification for d, which previously was assumed to be given by (5.22) with $\psi_3 = 0$. For purposes of obtaining a simple solution of (5.21) for θ_T, we make the further approximation (which is consistent with the data of Laufer 1951) that

$$d\frac{\partial\psi_1}{\partial x_2} = -\frac{4\sqrt{2}\psi_2\mu_8}{\mu_6}. \tag{5.30}$$

Substituting (5.30) into (5.21), after again neglecting the diffusion terms, assuming that the production of turbulent fluctuations is now completely controlled by the term possessing the highest power of d, and using the previously mentioned constitutive expressions for μ_8, ψ_1 and ψ_2, we obtain

$$\rho c_1 \rho_E^{\frac{1}{2}} \theta_T^{\frac{3}{2}} = 32\frac{\nu_1}{\rho_E}\left(\frac{\rho^2 c_7 c_5^2}{c_4 \mu_6^2}\right)^2 \theta_T^5 \left(\frac{\partial\theta_T}{\partial x_2}\right)^{-2}. \tag{5.31}$$

Taking the square root of (5.31) and integrating the resulting equation once with respect to x_2, after rearrangements gives a solution for θ_T of the form

$$\theta_T = \left[C - 3\sqrt{2}\left(\frac{\rho^{\frac{3}{2}}\,\nu_1^{\frac{1}{2}}\,c_7\,c_5^2}{c_1^{\frac{1}{2}}\,\rho_E^{\frac{3}{4}}\,c_4\,\mu_6^2}\right)x_2\right]^{-\frac{4}{3}}, \tag{5.32}$$

where C is another constant of integration.

(iv) *Results*

After appropriate selection of the response constants and specification of the various boundary conditions, the solutions (5.27), (5.29) and (5.32) for θ_T are plotted in figure 2 in their respective regions and are found to compare quite well with the data of Laufer (1951), both with regard to their numerical values and their functional forms. Using these solutions for θ_T, the velocity $\boldsymbol{v}$ is determined with the help of (5.19) and (5.22) and is plotted in figure 3 along with Laufer's 'mean velocity' data. The solution obtained here for v compares well with the data of Laufer, although very near the wall the slope in v is considerably less than that obtained experimentally. This deviation may be attributed to the fact that the term involving ψ_3 in (5.20) has been neglected in the approximation (5.22). The director is expected to become large along the wall and the effect associated with the term involving ψ_3 in (5.20) will necessarily increase the values of d and $\partial v/\partial x_2$ over those given by (5.22) and (5.19) in the region bordering the wall.

During the course of comparison of these solutions with the data of Laufer, values are necessarily assumed for certain of the response constants. Some of these constants, namely c_1 and c_3, are chosen so that expressions for dissipation and diffusion of turbulent fluctuations

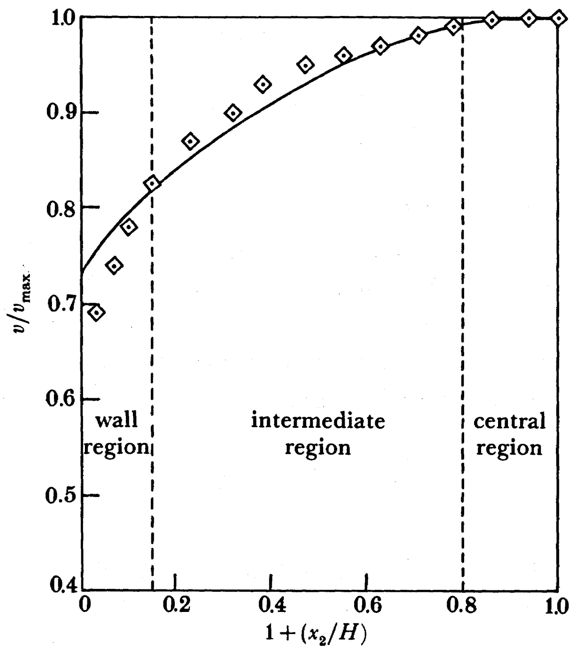

FIGURE 3. A plot of the macroscopic velocity profile v/v_{max} along the half-depth of the channel $-H \leqslant x_2 \leqslant 0$ for plane Poiseuille flow according to the approximate solution of § 5.4 and its comparison with corresponding data of Laufer (1951). The deviation between prediction of the theory and experiment should be attributed to the nature of the approximate solution near the wall region.

obtained previously are consistent with the estimates for these terms given by Laufer (1951, p. 1264, fig. 27). For other of the coefficients, the data necessary for such a term-wise comparison is not available. In plotting the curves in figures 2 and 3, the following values of the response constants are assumed:

$$\left.\begin{aligned} c_1 &= 5.82\times 10^{-6}\ \mathrm{m}^{\frac{7}{2}}\cdot{}^{\circ}T^{-\frac{3}{2}}\cdot\mathrm{s}^{-3},\\ c_3 &= 1.54\times 10^{-3}\ \mathrm{kg}\cdot\mathrm{m}^{\frac{1}{4}}\cdot{}^{\circ}T^{-\frac{3}{2}}\cdot\mathrm{s}^{-3},\\ c_7 &= 2.17\ \mathrm{m}^{\frac{1}{2}}\cdot{}^{\circ}T^{-\frac{1}{2}}\cdot\mathrm{s}^{-1},\quad \nu_1/\mu_6 = 6.8\times 10^{-5},\\ c_5/\mu_6 &= 0.61\ \mathrm{m}^{3}\cdot{}^{\circ}T^{-1}\cdot\mathrm{s}^{-1}\cdot\mathrm{kg}^{-1},\\ c_4^2/\mu_6 &\approx 10^{-7}\ \mathrm{m}^{7}\cdot{}^{\circ}T^{-2}\cdot\mathrm{s}^{-3}\cdot\mathrm{kg}^{-1}. \end{aligned}\right\} \tag{5.33}$$

In fully developed channel flows, such as that considered here, it is not necessary to make an explicit assumption for the coefficient μ_6; however, in other flows with non-vanishing inertia terms in (3.6) and (3.7), this would not necessarily be true. It is important to emphasize that the choices (5.33) are tentative and are recorded here for completeness.

Finally, plots of the approximate solution for the director magnitude d using (5.22), both before and after being multiplied by the turbulent temperature gradient, are shown in figure 4. It is of interest to note that the solution for d in (5.22) becomes unbounded along the centreline $x_2 = 0$. This dilemma is again caused by the fact that the term involving ψ_3 in (5.20) is neglected in the present discussion, so that the condition that $\partial d/\partial x_2$ vanishes along $x_2 = 0$

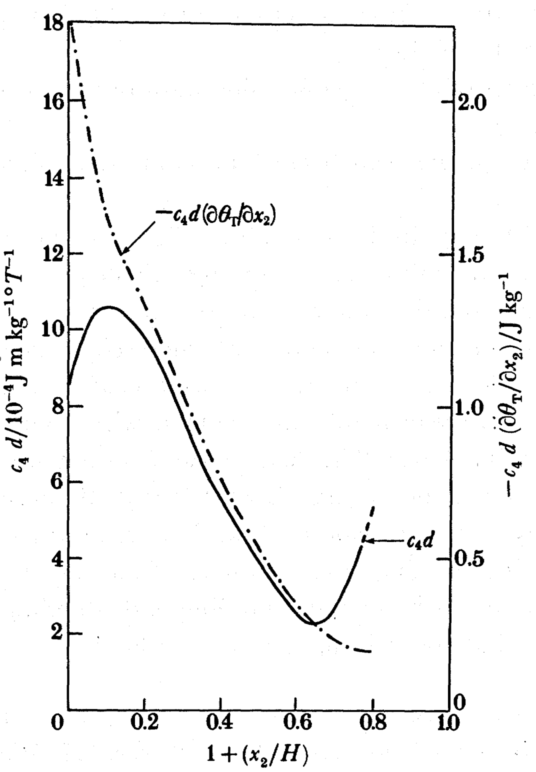

FIGURE 4. Estimated variation of the magnitude of the director d and the product $d(\partial\theta_T/\partial x_2)$ along the half-width of the channel against $1+(x_2/H)$ according to the approximate solution of §5.4.

cannot be applied. Although we would not expect (5.22) to yield reliable values for d either near the wall, as mentioned previously, or near the centre of the channel, the values obtained in the intermediate region $(0.15 \leqslant 1+x_2/H \leqslant 0.80)$ appear to be reasonable.

6. Concluding remarks

Comprehensive comparison of predictions of the theory presented in this paper and in I with experimental data and numerical simulations are necessary in order to both verify and complete the forms motivated in §4 for the response coefficients, as well as to determine additional constitutive relations for the supply terms appearing in the jump conditions in Part I (§7). These supply terms may then be used in conjunction with the appropriate jump conditions, to predict the boundary conditions on the independent variables along a surface of discontinuity. A first attempt for such a comparison in the case of plane turbulent Poiseuille flow is made in §5.4 of this paper. Although we are able to obtain a rough estimate for ρ_E from the data of Laufer (1951) for this problem, this data is not sufficiently detailed so as to enable similar estimates for d; and so the findings of §5.4, while encouraging, must be regarded as somewhat tentative. With such goals in mind, we now consider certain measurements that, if provided by future experimental data and/or numerical simulations, would both contribute to our general understanding of turbulent flow phenomena and enhance further development of the present theory.

As is discussed in §2, the additional turbulence variables utilized in this study are directly related to certain physically relevant features occurring on the microscopic scale of motion. Particular microscopic features whose measurements would allow proper determination of ρ_E and d may be summarized as follows:

(1) the number of eddies of class 2 (containing most of the 'turbulent kinetic energy') per unit volume (see §2.3);

(2) the number of those eddies which are (approximately) aligned in the direction $\boldsymbol{a}^3$ per unit volume (see §2.4);

(3) the typical vorticity magnitude ω^* of an unaligned eddy; and

(4) the typical vorticity magnitude ω^a of an aligned eddy.

There has been a considerable amount of recent interest in macroscopic turbulence modelling based upon idealization of significant microscopic flow structures. Although the instrumentation necessary to measure the relevant aspects of these structures (and in particular the four items listed above) were probably not available when many of the classic experimental studies were performed, it is believed that such instrumentation is either available today or will soon become so; in this connection, see also Laufer (1975). Because measurements of this type relate to the basic underlying structure of the flow, they are pertinent not only to measurements relating to the independent variables and character of the response functions in macroscopic theories of this sort, but also to a basic understanding of the fundamental physical mechanisms on the microscopic scale that control the macroscopic flow.

The results reported here were obtained in the course of research supported by the U.S. Office of Naval Research under Contract N00014-86-K-0057, Work Unit 4322534 with the University of California, Berkeley.

References

Ahlborn, B., Ahlborn, F. & Loewen, S. 1985 A model for turbulence based on rate equations. *J. Phys.* D **18**, 2127–2141.

Balint, J. L., Vukoslavĉevíc, P. & Wallace, J. M. 1986 A study of the vortical structure of the turbulent boundary layer. In *Advances in turbulence*, pp. 456–464. Berlin: Springer-Verlag.

Batchelor, G. K. 1952 *The theory of homogeneous turbulence*. Cambridge University Press.

Batchelor, G. K. 1967 *An introduction to fluid dynamics*. Cambridge University Press.

Bradshaw, P. 1987 Turbulent secondary flows. *A. Rev. Fluid Mech.* **19**, 53–74.

Champagne, F. H., Harris, V. G. & Corrsin, S. 1970 Experiments on nearly homogeneous turbulent shear flow. *J. Fluid Mech.* **41**, 81–139.

Comte-Bellot, G. & Corrsin, S. 1966 The use of a contraction to improve the isotropy of grid turbulence. *J. Fluid Mech.* **25**, 657–682.

Gad-el-hak, M. & Corrsin, S. 1974 Measurements of the nearly isotropic turbulence behind a uniform jet grid. *J. Fluid Mech.* **62**, 115–143.

Green, A. E. & Naghdi, P. M. 1977 On thermodynamics and the nature of the second law. *Proc. R. Soc. Lond.* A **357**, 253–270.

Head, M. R. & Bandyopadhyay, P. 1981 New aspects of turbulent boundary-layer structure. *J. Fluid Mech.* **107**, 297–338.

Kim, J., Moin, P. & Moser, R. 1987 Turbulence statistics in fully developed channel flow at low Reynolds number. *J. Fluid Mech.* **177**, 133–166.

Laufer, J. 1951 Investigation of turbulent flow in a two-dimensional channel. Natn Adv. Comm. Aeronautics, Wash., D.C. Report no. 1053, pp. 1247–1265.

Laufer, J. 1954 The structure of turbulence in fully developed pipe flow. Natn Adv. Comm. Aeronautics, Wash., D.C., Report no. 1174, pp. 417–434.

Laufer, J. 1975 New trends in experimental turbulence research. *A. Rev. Fluid Mech.* **7**, 307–326.

Liu, N. S., Shamroth, S. J. & McDonald, H. 1985 On hairpin vortices as model of wall turbulence structure. In *Proc. 5th Turbulent Shear Flows Symp, Ithaca, New York.*

Marshall, J. S. & Naghdi, P. M. 1988 A thermodynamical theory of turbulence. I. Basic developments. *Phil. Trans. R. Soc. Lond.* A **327**, 415–448. (Preceding paper.)

Mumford, J. C. 1983 The structure of large eddies in fully developed turbulent shear flows. Part 2. The plane wake. *J. Fluid Mech.* **137**, 447–456.

Perry, A. E. & Chong, M. S. 1982 On the mechanism of wall turbulence. *J. Fluid Mech.* **119**, 173–217.

Prandtl, L. 1925 Bericht über Untersuchungen zur ausgebildeten Turbulenz. *Z. angew. Math. Mech.* **5**, 136–139.

Prandtl, L. & Tietjens, O. G. 1957 *Fundamentals of hydro- and aeromechanics*. New York: Dover.

Reynolds, W. C. 1976 Computation of turbulent flows. *A. Rev. Fluid Mech.* **8**, 183–208.

Rogers, M. M. & Moin, P. 1987 The structure of the vorticity field in homogeneous turbulent flows. *J. Fluid Mech.* **176**, 33–66.

Savill, A. M. 1987 Recent developments in rapid-distortion theory. *A. Rev. Fluid Mech.* **19**, 531–575.

Tennekes, H. & Lumley, J. L. 1972 *A first course in turbulence*. Cambridge, Massachusetts: MIT Press.

Townsend, A. A. 1954 The uniform distortion of homogeneous turbulence. *Q. Jl Mech. appl. Math.* **7**, 104–127.

Townsend, A. A. 1956 *The structure of turbulent shear flow*, 1st edn. Cambridge University Press.

Townsend, A. A. 1976 *The structure of turbulent shear flow*, 2nd edn. Cambridge University Press.

Townsend, A. A. 1979 Flow patterns of large eddies in a wake and in a boundary layer. *J. Fluid Mech.* **95**, 515–537.

Tucker, H. J. & Reynolds, A. J. 1968 The distortion of turbulence by irrotational plane strain. *J. Fluid Mech.* **32**, 657–673.

Uberoi, M. S. 1956 Effect of wind-tunnel contraction on free-stream turbulence. *J. aeronaut. Sci.* **23**, 754–764.